Detection of variations in cognitive workload using multi-modality physiological sensors and a large margin unbiased regression machine

Haihong Zhang and Yongwei Zhu and Jayachandran Maniyeri and Cuntai Guan

Abstract— **Physiological sensor based workload estimation technology provides a real-time means for assessing cognitive workload and has a broad range of applications in cognitive ergonomics, mental health monitoring, etc. In this paper we report a study on detecting changes in workload using multi-modality physiological sensors and a novel feature extraction and classification algorithm. We conducted a cognitive workload experiment involving multiple subjects and collected an extensive data set of EEG, ECG and GSR signals. We show that the GSR signal is consistent with the variations of cognitive workload in 75% of the samples. To explore cardiac patterns in ECG that are potentially correlated with the cognitive workload process, we computed various heart-rate-variability features. To extract neuronal activity patterns in EEG related to cognitive workload, we introduced a filter bank common spatial pattern filtering technique. As there can be large variations in e.g. individual responses to the cognitive workload, we propose a large margin unbiased recursive feature extraction and regression method. Our leave-one-subject-out cross validation test shows that, using the proposed method, EEG can provide significantly better prediction of the cognitive workload variation than ECG, with 87.5% vs 62.5% in accuracy rate.**

I. INTRODUCTION

Cognitive workload, the level of mental resources required of a person at a time, affects human ability in information processing and decision making. Therefore, it is an important cognitive science discipline with a wide range of applications, e.g. cognitive ergonomics to optimize human well-being and system performance [1] [2].

An emerging approach to cognitive workload assessment is through computing various physiological signals, which allows real-time and unobstrusive monitoring in constrast to conventional but obstrusive measures using user (and/or expert) reports such as NASA-TLX [3]. For example, heart rate variability (HRV) has been connected to mental effort in human computer interaction in [4]. Galvanic skin response (GSR) has also been correlated with levels of cognitive processing [5]. Electroencephalogram (EEG) studies have also demonstrated that specific rhythmic powers are correlated with difficulty level of cognitive tasks such as n-back and flight simulation tasks [6]. Recently in [7], EEG analysis of cortical connective networks was also used to differentiate specific mental arithmetic tasks.

However, it is still an open question how to precisely assess cognitive workload using the physiological signals that are subject to large variability over time and across subjects [8], [9]. While multi-channel EEG was employed in various prior studies, usually only individual channels were investigated separately. Compared to joint analysis of multiple channels, individual channel analysis tends to be more prone to variability, because of limited information and poor spatial specificity and low signal-to-noise ratio of EEG. Another open question is that, due to inter subject variability, the individual response to the workload may vary largely from person to person; and this may affect the accuracy of cognitive assessment tools.

The present work consists of a new attempt to address the abovementioned issues. First, we introduce a fiter bank common spatial pattern filtering technique to identify and extract cognitive workload-related spatial-spectral signatures in multi-channel EEG. Second, to address the varibility of individual's physiological response to cognitive workloads, we designed a large margin unbiased regression machine. We have conducted a cognitive workload experiments and used 16 subjects with complete data recordings in an offline study with leave-one-subject-out cross validation. The result indicates that change of cognitive workload can be detected in all the physiological signals including GSR, EEG and heart rate. Especially, the cross validation test shows that the EEG features provide better prediction of the cognitive workload variation than both single-channel EEG features and HRV features.

II. COGNITIVE WORKLOAD DATA SET

In this work we recruited healthy adult subjects who gave written constents to participate in the study which was ethically approved by the National University of Singapore Institutional Review Board beforehand. The subjects were placed on a comfortable chair. A PPG device connected to multiple sensors attached to the subjects and the following signals were acquired: electrocardiogram (ECG), GSR, SpO2 (not used in this study). A separate EEG amplifier of Neuroscan connected to a full-head EEG cap of 40-channels referenced to the right mastoid. This study used 15 channels only, namely, F3, Fz, F4 , FC3, FCz, FC4, C3, Cz, C4, CP3, CPz, CP4, P3, Pz, P4.

The cognitive workload procedure consisted of the following stages. In the first stage, the subjects were resting in the chair for 5 minutes. In the second stage, the subjects received a sequence of 6 cognitive tasks on cognitivefun.net, including Go/No-go visual reaction test, stroop test, fast counting test, speed run test, visual forward digit span test, and working memory test. The whole sequence of cognitive workload lasted 30 minutes for each subject. In the third stage, the

The authors are with the Neural and Biomedical Technology Department, Institute for Infocomm Research, Agency for Science, Technology and Research, Singapore hhzhang at i2r.a-star.edu.sg

978-1-4244-7929-0/14/$26.00 ©2014 IEEE

subjects relaxed for 10 minutes. Throughout the procedure any excessive movement was not allowed.

We performed data screening and rejecting of subjects' data which were affected by recording errors or signal quality issues. There were 16 subjects' data left for this study.

III. Proposed EEG-based workload measure

We consider discriminative spatial-spectral EEG components in relation to different workload conditions. The spectral contents in EEG indicate specific macroscopic neural oscillations, and the common rhythmic activity frequency bands are well defined [10]. On the other hand, EEG suffers poor spatial resolution and high noise level, while spatial filtering provides an effective means for improving spatial specificity and signal-to-noise ratio [11]. In this work, we adapt a method developed in [12] to extract discriminative spatial-spectral EEG components that contrast EEG between the different workload conditions presented in the data. This method is described in the subsection below.

In the subsection thereafter, we also propose a new recursive feature selection and regression algorithm. We discuss the justifications for unbiased regression for mapping features into contrasting cognitive workload states.

Here we would like to emphasize that this work links the workload assessment to a special binary classification problem. Two contrasting classes are the resting-to-workload class ω_1 (i.e. from the first stage to the second stage in the above protocol), and the workload-to-resting class ω_1 (i.e. from the second to the third stage in the above protocol).

A. Joint spatial-spectral feature extraction

Let's consider the spatial-spectral filtering in the spectral domain, where an n_c-channel EEG segment with a sampling rate of F_s-Hz can described by an $n_c \times n_f$ matrix.

$$\mathbf{X} = \begin{bmatrix} x_{11} & \cdots & x_{1n_f} \\ \vdots & \ddots & \vdots \\ x_{n_c1} & \cdots & x_{n_cn_f} \end{bmatrix} \tag{1}$$

where x_{ij} denotes the discrete Fourier transform of the i-th channel at frequency $\omega_j = \frac{j-1}{2n_f}F_s$.

A joint spatial-spectral filter on $\mathbf{X}$ can be essentially represented by a spatial filtering vector $\mathbf{w} \in \mathbb{R}^{n_c \times 1}$ and a spectral filter vector $\mathbf{f} \in \mathbb{R}^{n_f \times 1}$. As there can be multiple interesting rhythmic components in EEG, we need to examine each and every EEG frequency bands possibly related, including *theta* (4-7Hz), *alpha*(7-13Hz), *low beta*(12-16Hz), *mid beta* (16-20Hz), and *high-beta* (20-28Hz). And we set f to be a window function specific for each band, with its element being 1 if within the band or being 0 otherwise.

The feature g representing the EEG rhythmic power of a spatial component is

$$g = \frac{1}{T}\text{diag}\left\{\widetilde{\mathbf{w}^T\mathbf{X}}\left(\mathbf{w}^T\mathbf{X}\right)\right\}\mathbf{f} \tag{2}$$

where T is the duration of the EEG signal, the wave line $\widetilde{}$ on the right side of the equation denotes the conjugate of a complex value, and the diag() function stands for the diagonal vector of a matrix.

And the spatial filter is constructed to contrast two classes by minimizing or maximizing the Rayleigh quotient [13] (see [14] for a Bayesian spatial filtering analysis related to Rayleigh quotient).

$$\frac{\mathbf{w}^T\mathbf{E}[\mathbf{R}|\omega_1]\mathbf{w}}{\mathbf{w}^T\mathbf{E}[\mathbf{R}|\omega_2]\mathbf{w}} \tag{3}$$

where $\mathbf{E}$ means the expectation operator and $\mathbf{R}$ is the covariance matrix of the EEG signal. The minimization can be solved using a generalized eigen value solution [11].

Therefore, for each of the four frequency bands, we construct two spatial filters that maximizing or minimizing the Rayleigh quotient. In total there are 8 features from the spatial-spectral filtering method.

B. Modelling the workload states in the feature space

A traditional way to measure the workload is by contructing a regression function that maps the feature vector to a workload metric. However, due to large variations across subjects, the mapping function may vary considerably and a single physical model may not suffice to represent all. On the other hand, in many workload cases like in our protocol, there are only, strictly speaking, three physiological workload samples from the three stages respectively, making it difficult to build a subject-specific model.

In view of the challenges, we resort to building subject-independent model that considers large variations between subjects. To this end, we design an unbiased regression approach in the following.

Let $\mathbf{g}$ the feature vector consisting elements of g. A linear regression that maps $\mathbf{g}$ to a workload metric $\hat{z}$ works by

$$\hat{z} = \mathbf{u}\mathbf{g} + b \tag{4}$$

where $\mathbf{u}$ is the linear coefficient vector and b the bias.

As discussed above, the bias b is subject to large variation between subjects. To eleminate the effect of b, we considers the change of workload metric instead of the absolute workload. In our data set, there were two cases of such change, one from the initial resting stage to the workload stage, the other from the workload stage to the final resting stage. So the problem can be formulated as finding the projection vector $\mathbf{u}$ that yields

$$cz = c \cdot \mathbf{u}^T d(\mathbf{g}) >= 0 \tag{5}$$

where $d(\mathbf{g})$ is the change of the feature vector in either of the abovementioned changes, c is -1 or 1 representing the resting-to-workload change, or the workload-to-resting change.

Following a similar precedure of large margin formulation to [15], we write the special zero-bias learning problem as

$$\min_{\mathbf{u}}[J(\mathbf{u}) = \frac{\lambda}{2}(\mathbf{u}^T\hat{\mathbf{G}}\hat{\mathbf{G}}^T\mathbf{u} + N - 2\mathbf{u}^T\hat{\mathbf{G}}\mathbf{C}\mathbf{e}) + \frac{1}{2}\mathbf{u}^T\mathbf{u}] \tag{6}$$

where λ ($\lambda = 1$ tentatively in this study) is a regularization coefficient, $\hat{\mathbf{G}}$ is the matrix of all $d(\mathbf{g})$ samples as column

vectors, N the number of samples, $\mathbf{C}$ is the diagonal matrix of c, $\mathbf{e}$ is the all 1 vector.

The solution to minimization of J is given by

$$\mathbf{u} = \left[\frac{1}{\lambda}\mathbf{I} + \hat{\mathbf{G}}\left(\mathbf{I} - \frac{1}{N}\mathbf{e}\mathbf{e}^T\right)\mathbf{X}^T\right]^{-1}\hat{\mathbf{G}}\mathbf{C}\mathbf{e} \qquad (7)$$

where $\mathbf{I}$ is the identity matrix.

Thus, for a given set of training samples $d(\mathbf{g})$, we designed a recursive feature selection and regression algorithm. The intial set of selected feature is null. The algorithm tests each and every of the feature, and uses Eq. 7 to learn the unbiased regress function coefficient vector $\mathbf{u}$. The best feature is choosen if it maximizes the correlation coefficient between the c vector and the regression result $z = \mathbf{u}^T d(\mathbf{g})$. Due to limited space, the detailed steps of the algorithm are omitted.

To examine the generalized performance of the method, we used an leave-one-subject-out validation approach. Specifically, we built a workload prediction model by using the data from the other subjects. In other words, each subject presented as a test sample and the other subjects as training samples.

IV. Data analysis and results

A. User ratings and GSR signal

Subjective ratings of stress were collected immediately after each data collection stage, using a widely used questionnaire called the State-Trait Anxiety Inventory (STAI). This questionnaire attempts to characterize two types of stress. The is characterized by feelings of anxiety caused by fear, nervousness, discomfort and arousal of the autonomic nervous system, hence termed state anxiety. This form of stress characterizes feelings at the time of perceived danger or threat, and is thus considered short term or temporary. The second form of stress is characterized by feelings of anxiety caused by stress, worry, discomfort etc. that one experiences on a daily basis. This form of stress characterizes feelings that make a person predisposed towards being stressed in particular ways, possibly because of factors that are longer term.

The change of the subjective ratings is illustrated in Figure 1 left panel. Apparently, 12 out of 16 subjects felt increased stress from Stage 1 (resting) to Stage 2 (cognitive tasks), while 10 subjects felt decreased stress from Stage 2 to Stage 3 (final resting).

The mean GSR value in each stage was computed and compared between different stages. The result is illustrated in Figure 1 right panel. As expected, all but one subjects produced lower GSR in Stage 2 than Stage 1, which can be attributed to an increase in perspiration due to the workload as well as the associated stress. Comparing Stage 3 to Stage 2, there were 12 subjects producing higher GSR, but there were 4 subjects did not show the expected GSR increase.

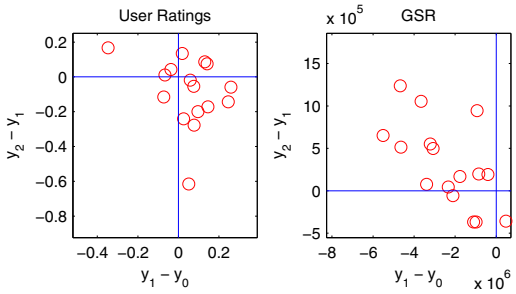

Fig. 1. Change of user stress ratings and GSR values. The x-axis represents the change of the score (user rating or GSR value) from Stage 1 to Stage 2 in the cognitive workload experiment, the y-axis from Stage 2 to Stage 3. Each data point represents a particular subject session.

B. Change of heart rate variability based workload prediction

Heart rate variability (HRV) features were computed from heart beat interval sequency in each stage. To measure HRV from ECG, the term RR interval is used, where R represents a time point corresponding to the peak of the QRS complex in ECG. When term NN is used in place of RR in HRV measurement, the emphasis is on the fact that the processed beats are normal beats. In this study, we considered 10 time-domain features only, including max, min, mean, median, SDNN: the standard deviation of NN intervals; SDSD: the standard deviation of the successive differences between adjacent NNs; NN50: the number of pairs of successive NNs that differ by more than 50 ms; pNN50: the proportion of NN50 divided by total number NNs; RMSSD: the square root of the mean of the sum of the squares of the successive differences between adjacent NNs. The HRV features were computed using the software provided at https://github.com/jramshur/HRVAS.

As we found that any individual HRV feature may not correlate with the workload variations, we used the same recuisive feature extraction and large margin unbiased regression machine, which is described in the previous section.

The result is illustrated in Figure 2. If using all subjects' data for training, the first three selected ECG features were TINN, MIN, and mean HR (bpm). It appears from the result that the second and the third selected features did not contribute much to workload measurement. With three features, the measurement shows increased workload level from Stage 1 to Stage 2 in 13 subjects, and decreased workload level from Stage 2 to Stage 3 in 11 subjects.

C. EEG features and workload prediction

For all the subjects as a whole, the proposed algorithm identified the top three features in high beta band, middle beta band and alpha band. In the illustration Figure 3, we can see that the majority contribution for workload measure comes from the first feature, i.e. the high beta band activity.

Furthermore, the above graphs indicate that the EEG-based workload measurement may predict with higher accuracy the variation of workload, especially from resting to cognitive

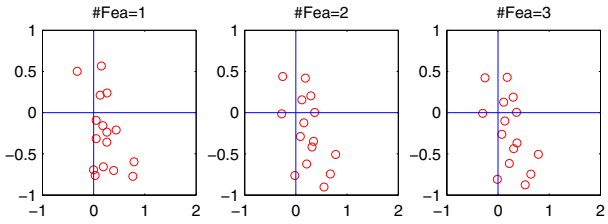

Fig. 2. Change of workload score predicted by heart rate viarability. Refer to Fig. 1 for the meaning of the axes. From left to right are the results with 1 selected feature, 2 selected features and 3 selected features from ECG data, respectively.

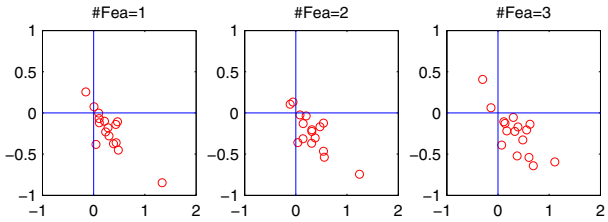

Fig. 3. Change of workload score predicted by EEG. Refer to Fig. 1 for the meaning of the axes. From left to right are the results with 1 selected feature, 2 selected features and 3 selected features from EEG data, respectively.

task and vice versa. In Table I, we give the prediction accuracy rate: the number of cases (subjects) for which the prediction gives increasing values from Stage 1 to 2 and also decreasing values from Stage 2 to 3. Apparently the EEG features based prediction gives the highest accuracy among the three.

TABLE I

COMPARATIVE ACCURACY OF WORKLOAD CHANGE PREDICTION. HRV FEATURES ARE EXTRACTED FROM 1-LEAD CHEST ECG.

Method	GSR	HRV	EEG
Accuracy	75%	62.5%	87.5%

V. CONCLUSION

In this paper we have reported a new study on multi-modality physiological signals in relation to variations of workload. Using discriminant spatial-spectral feature extraction and unbiased large margin regression, we have shown that EEG can predict the variations of workload condition with higher accuracy than what GSR or HRV can provide. As this is a preliminary study, the subjective rating method can be improved to be more specific for cognitive workload. Furthermore, we are further analyzing the EEG features (spatial-spectral components) as well as new related EEG features (such as connectivity) to further the understanding of EEG in relation to cognitive workload.

REFERENCES

[1] M. Just, P. Carpenter, and A. Miyake, "Neuroindices of cognitive workload: neuroimaging, pupillometric and event-related potential studies of brain work," *Theoretical Issues in Ergonomics Science*, vol. 4, no. 1-2, pp. 56–88, 2003.

[2] T. C. Hankins and G. F. Wilson, "A comparison of heart rate, eye activity, eeg and subjective measures of pilot mental workload during flight," *Aviation Space and Environmental Medicine*, vol. 69, no. 4, pp. 360–367, 1998.

[3] S. Hart, "Nasa-task load index (nasa-tlx): 20 years later," in *Human Factors and Ergonomics Society Annual Meeting Proceedings*, 2006, pp. 904–908.

[4] L. Izso and E. Lang, "Heart period variability as mental effort monitor in human computer interaction." *Behaviour & Information Technology*, vol. 19, no. 4, pp. 297–306., 2000.

[5] R. Cohen and W. Waters, "Psychophysiological correlates of levels and stages of cognitive processing," *Neuropsychologia*, vol. 23, no. 2, pp. 243–256, 1985.

[6] A. Gelvin and M. Smith, "Neurophysiological measures of cognitive workload during human-computer interaction," *Theoretical Issues in Ergonomics Science*, vol. 4, pp. 113–131, 2003.

[7] S. Dimitriadis, Y. Sun, K. Kwok, N. Laskaris, and A. Bezerianos, "A tensorial approach to access cognitive workload related to mental arithmetic from eeg functional connectivity estimates," in *Annual Inernational Conference of the IEEE EMBS*, 2013.

[8] G. F. Wilson, J. Estepp, and J. Christensen, "How does day-to-day viariability in psychophysiological data affect classifier accuracy," in *Human Factors and Ergonomics Society Annual Meeting Proceedings*, 2009, pp. 264–268.

[9] D. T. Jones, P. Vemuri, M. C. Murphy, J. L. Gunter, M. L. Senjem, M. M. Machulda, S. A. Przybelski, B. E. Gregg, K. Kantarci, D. S. Knopman, B. F. Boeve, R. C. Petersen, and C. R. Jack, Jr, "Non-stationarity in the "resting brains" modular architecture," *PLoS ONE*, vol. 7, no. 6, p. e39731, 06 2012.

[10] E. Niedermeyer and F. da Silva, Eds., *Electroencephalography: Basic Principles, Clinical Applications, and Related Fields*. Lippincot Williams & Wilkins, 2004.

[11] B. Blankertz, R. Tomioka, S. Lemm, M. Kawanabe, and K.-R. Müller, "Optimizing spatial filters for robust EEG single-trial analysis," *IEEE Signal Processing Magazine*, vol. 25, pp. 41–56, 2008.

[12] K. K. Ang, Z. Y. Chin, H. Zhang, and C. Guan, "Filter bank common spatial pattern (FBCSP) in brain-computer interface," in *International Joint Conference on Neural Networks (IJCNN2008)*, 2008, pp. 2391–2398.

[13] R. A. Horn and C. A. Johnson, Eds., *Matrix Analysis*. Cambridge University Press, 1985.

[14] H. Zhang and C. Guan, "Bayesian learning for spatial filtering in eeg-based brain-computer interface," *IEEE Transactions on Neural Networks and Learning Systems*, vol. 7, pp. 1–12, 2013.

[15] F. A. C. de Bastos and M. L. R. de Campos, "A fast training algorithm for unbiased proximal svm," in *ICASSP*, 2005.